example, the electron temperature of a hot plasma generating hard radiation by Compton collisions) cannot be easily maintained in neutron star systems where strong, low-energy emission from the star surface would cool the plasma by Compton scattering[10]. The soft group (hardness ratio $\leqslant 0.6$), includes four genuine neutron-star binaries: one accreting X-ray pulsar, and three X-ray bursters. These sources have already been reported to feature sporadic hard X-ray emission, but our analysis shows now that they must actually be considered nearly persistent sources of hard X-rays, systematically fainter and softer than black hole candidates. Using the estimate of the hardness ratio as a criterion to distinguish the nature of hard X-ray emitting compact objects, we propose that the two sources SLX1735−269 and GRS1743−290 are also accreting neutron stars. Note also that the sporadic broad high-energy feature observed on three occasions by Sigma from 1E1740.7−2942 (refs 12–14) and probably related to positron annihilation processes substantiates the hypothesis of the black-hole nature of this source.

An important result of the Sigma deep survey of the Galactic Centre is that the Galactic nucleus is silent above 35 keV. Although in the 75–150 keV band, the 1990–93 average luminosity is definitely $<2.4\times10^{35}$ erg s^{-1} (2σ upper limit for a distance of 8.5 kpc), it is more difficult to determine such a compelling limit in the 35–75 keV band, because of the presence of the nearby source GRS1743−290. Although we can reject the hypothesis that Sgr A* is the counterpart of GRS1743−290 (probability $<10^{-5}$ for two degrees of freedom), the upper limit of the 35–75 keV luminosity of the Galactic nucleus cannot be set below 3.5×10^{35} erg s^{-1}. These limits can be compared to the nearly contemporary data obtained by ART-P during autumn 1990 (ref. 6). The rather flat spectrum ($\alpha=1.6$) of Sgr A* measured by ART-P (and extrapolated to the adopted Sigma energy bands) implies luminosities respectively 3 and 5.7 times higher than the quoted upper limits in the 35–75 and the 75–150 keV bands. Even considering the uncertainties in the ART-P spectrum, our data imply a break in the Sgr A* X-ray spectrum at a critical energy, probably between 20 and 40 keV. As a consequence, the total 3–150 keV luminosity of Sgr A* cannot exceed 2.5×10^{36} erg s^{-1}, a value which must be compared to the Eddington luminosity of a black hole of 10^6 solar masses that is, $\sim10^{44}$ erg s^{-1}. In the hypothesis that a massive black hole at the Galactic nucleus accretes matter from the close ($\sim$0.04 pc) hot star cluster IRS156 via powerful stellar winds, the limit on the black hole mass which can be derived from our hard X-ray upper limits, and from the break we predict in the X-ray spectrum, is still rather controversial[25,26], because it depends strongly on the assumptions made about the model and radiation mechanisms. Our results definitely show that if an accreting massive black hole resides at the Galactic nucleus, it does not efficiently convert to hard X-ray and soft γ-rays the potential energy provided by accretion of the IRS16 star-cluster wind, and it clearly does not behave like a scaled-down active galactic nucleus. In addition, past detection of a variable narrow 511 keV line emission from the Galactic Centre region, although not localized, has often supported the belief that a massive black hole resides in the Galactic nucleus[1]. The lack of 511 keV line detection from the Galactic nucleus itself—a Sigma upper limit of 2.45×10^{-4} photons cm^{-2} s^{-1} has been obtained for both 1E1740.7−2942 and Sgr A* (ref. 27)—does not rule out the possible presence of a weak compact variable 511 keV source, but certainly implies that the Galactic nucleus remains underluminous at the electron–positron annihilation energy. □

Received 1 June; accepted 8 September 1994.

1. Genzel, R. & Townes, C. H. *A. Rev. Astr. Astrophys.* **25,** 377–423 (1987).
2. Gehrels, N. & Tueller, J. *Astrophys. J.* **407,** 597–605 (1993).
3. Watson, M. G., Willingale, R., Grindlay, J. & Hertz, P. *Astrophys. J.* **250,** 142–154 (1981).
4. Skinner, G. K. *et al. Nature* **330,** 544–547 (1987).
5. Hertz, P. & Grindlay, J. E. *Astrophys. J.* **278,** 137–149 (1984).
6. Pavlinsky, M. N., Grebenev, S. A. & Sunyaev, R. *Astrophys. J.* **425,** 110–121 (1994).
7. Paul, J. *et al. Adv. Space Res.* **11,** 289–302 (1991).
8. Cook, W. R. *et al. Astrophys. J.* **372,** L75–L78 (1991).
9. Covault, C., Manandhar, R. & Grindlay, J. *Proc. 22nd Int. Cosmic Ray Conf.* Dublin Vol. 1 21–24 (1991).
10. Sunyaev, R. *et al. Astr. Astrophys.* **247,** L29–L32 (1991).
11. Cordier, B. *et al. Astr. Astrophys.* **272,** 277–284 (1993).
12. Bouchet, L. *et al. Astrophys. J.* **383,** L45–L48 (1991).
13. Sunyaev, R. *et al. Astrophys. J.* **383,** L49–L52 (1991).
14. Cordier, B. *et al. Astr. Astrophys.* **275,** L1–L4 (1993).
15. Gilfanov, M. *et al. Astrophys. J.* **418,** 844–849 (1993).
16. Goldwurm, A. in *Proc. of Capri Workshop on Imaging in High Energy Astronomy* (eds Bassani, L. & Di Cocco, G.) (Bologna, Italy, in the press).
17. Gilfanov, M. *et al. in Proc. 4th A. Astr. Maryland Conf.* College Park, Maryland, USA (in the press).
18. Barret, D. *et al. Astrophys. J.* **379,** L21–L24 (1991).
19. Claret, A. *et al. Astrophys. J.* **423,** 436–440 (1994).
20. Laurent, P. *et al. Astr. Astrophys.* **278,** 444–448 (1993).
21. Churazov, E. *et al. Astrophys. J. Suppl. Ser.* **92,** 381–385 (1994).
22. Zhao, J. *et al. Science* **255,** 1538–1543 (1992).
23. Cox, P. & Laureijs, R. in *The Center of the Galaxy* (ed. Morris, M.) 121–128 (IAU Kluwer, Symp. No. 136, Dordrecht, 1989).
24. Markevitch, M., Sunyaev, R. A. & Pavlinsky, M. N. *Nature* **364,** 40–42 (1993).
25. Mastichiadis, A. & Ozernoy, L. M. *Astrophys. J.* **426,** 599–603 (1994).
26. Melia, F. *Astrophys. J.* **426,** 577–585 (1994).
27. Malet, I. *et al. Astrophys. J.* (in the press).

ACKNOWLEDGEMENTS. We acknowledge the vital contribution of the CNES Toulouse Space Centre to this work, and thank the staff at the Lavotchine Space Company, the Babakin Space Centre, the Baikonour Space Centre and the Evpatoria Ground Station for their unfailing support.

An organic solid with wide channels based on hydrogen bonding between macrocycles

D. Venkataraman*, Stephen Lee†‡, Jinshan Zhang†§ & Jeffrey S. Moore*‡

* Departments of Chemistry and Materials Science & Engineering, University of Illinois, Urbana, Illinois 61801, USA
† Department of Chemistry, University of Michigan, Ann Arbor, Michigan 48109, USA

RESEARCH on microporous solids has focused largely on inorganic materials such as aluminosilicates (zeolites), aluminophosphates, pillared clays and other layered materials[1,2]. An elusive goal has been the design of new materials with specific properties such as selective adsorption and catalytic activity. It would be very useful if the tools of molecular synthesis could be brought to bear on this problem. Here we report the design, based on a modular approach, and the crystal structure of an organic solid with large-diameter (about 9 Å) extended channels. The channels are formed from planar, rigid macrocyclic building blocks. Onto the outer rim of the macrocycles are attached phenolic groups, which form hexagonally closest-packed two-dimensional hydrogen-bonded networks. Extended channels result from the stacking of these layers in a way that maintains registry between the macrocyclic cavities, and these channels are filled with solvent molecules. This approach potentially offers a simple means to exercise control over pore size and shape in the solid state.

One of the difficulties in applying the methodology of organic chemistry to the design of porous solids is the isotropic nature of intermolecular interactions of organic molecules. This isotropy generally leads to closest packings. Work has been carried out on the use of more directional intermolecular interactions, such as hydrogen bonds, to control solid-state organization[3–7]. Many examples of one-dimensional chains as well as two- and three-dimensional hydrogen-bonded networks are known. Networks have even been designed with the intention of creating large cavities; however, in the solid state the networks tend to self-

‡ Authors to whom correspondence should be addressed.
§ Present address; Motorola Inc., 8000 West Sunrise Boulevard, Fort Lauderdale, Florida 33322, USA.

interpenetrate, filling the voids left in the initial host structure[8–13]. Generally the end result is a dense structure, although a nanoporous coordination network was reported recently by Abrahams *et al.*[14]. Solid-state organic hosts which enclose guests in extended channels are well known, but usually these channels are formed by intermolecular packing voids which happen to lie along a common axis[15,16]. Only a small number of tubular clathrates are known in which the walls of the channel are formed by the interior of a macrocyclic building block[17–19].

We suggest that a promising approach to molecular-based porous crystals would involve the use of high-symmetry, multi-coordinating macrocycles made of stiff units that resist buckling even in the solid state. Depending on the nature of the macrocycle, even closest-packed motifs of such building blocks could exhibit significant porosity, with the added advantage that closest packing would prevent interpenetration. Hence macrocycle **1** (Fig. 1) with phenolic groups on the exterior was synthesized[20], with the expectation that the phenolic groups would organize intermolecular hydrogen bonding, leading to a two-dimensional hexagonal network. Based on the known aggregation behaviour[21,22] of the macrocycles, it was postulated that these layers might pack atop one another in such a fashion that extended channel structures would be generated.

Crystals were grown by the slow diffusion of methanol into a solution of **1** in ethanol in a 1-mm sealed capillary tube. The lattice was found to be trigonal with cell dimensions $a=20.660\ (8)$ and $c=9.998\ (7)$ Å. The systematic extinctions, together with R_{merge}, showed the space group to be $P3_1$ (no. 144) or equivalently $P3_2$ (no. 145). As the molecular itself is a toroid of approximately $18\times18\times3.5$ Å, it is clear by comparison to the unit cell dimensions that no more than three molecules can occupy the primitive cell. Furthermore, as there is only one site of symmetry in $P3_2$, and this site has 3-fold multiplicity, we concluded that there is only one crystallographically inequivalent molecule per unit cell. The orientation of this single molecule can be unambiguously deduced from the Patterson function (note that as the molecule is of D_{6h} symmetry and as the molecules lie normal to the c axis, all bonds of **1** are in the same directions of the Patterson map). Molecule **1** is nearly rigid, and so the only remaining variables needed for an initial solution were the x and y coordinates of the centre of the crystallographically inequivalent molecule. They were determined by systematic trial and error. Allowing the molecule to relax from a perfectly planar geometry resulted in an R factor (R_1) of 32.4%. At this point, solvent molecules consisting of 12 ethanol, 6 methanol and 3 water molecules appeared in the Fourier map (Fig. 2). The density observed by the flotation method was close to the calculated density (calculated, 1.29 g cm^{-3}; observed, 1.24 g cm^{-3}). Solvent molecules were at positions compatible with hydrogen bonding to the hexaphenol and with reasonable bond distances and bond angles for ethanol and methanol. Disorder in the solvent atoms was apparent from their thermal parameters, especially for those carbons furthest removed from the hydrogen-bonded oxygen. The disorder observed in the solvent is in sharp contrast to macrocyclic atoms which were well resolved in subsequent electron density maps. Isotropic refinement led to a final R_1 factor of 17.58 for 2,391 reflections ($F>4.0\sigma$) and 130 parameters (Table 1)[23]. The bond angles and distances are in accord with the chemical structure of the molecule. The Fourier difference map showed a residual electron density of 0.67 electrons Å^{-3}.

TABLE 1 Crystal data for compound **1** at −140 °C

Crystal system	Trigonal
Space group	$P3_1(144)$ or $P3_2(145)$
Cell parameters	$a=b=20.660\ (9)$ Å
	$c=9.998\ (7)$ Å
	$\alpha=\beta=90°$
	$\gamma=120°$
Z	3
Volume	3,695.5 (33) Å^3
Octants used for data collection	Full sphere
No. of reflections refined	2,704
No. of parameters	130
Unweighted agreement factor (R_1)	0.1758 ($F>4\sigma$)
	0.1816 (all data)
Highest peak in the final difference map	0.67 electrons per Å^3
Goodness of fit	1.157

Experimental details: diffractometer, Syntex $P2_1$ IV; Mo μ λ(Mo Kα) = 0.075 mm^{-1}; (Mo Kα) = 0.710734 Å, Lp corrected; 8,246 reflections collected; number of reflections >4.0 (σ (f) = 2,391; computing structure solution, SHELXTL PLUS; computing structure refinement, SHELXL-93; reflections were refined based on F_0^2 by full matrix least-squares.

The structure is layered, with each layer consisting of sheets of macrocycles hydrogen-bonded to one another forming a two-dimensional closest-packed structure (Fig. 1). Of the two common types of aromatic packing modes[24], namely the stack and herringbone patterns, efficient packing in the latter is prevented by the topological constraints of macrocyclization and the drive

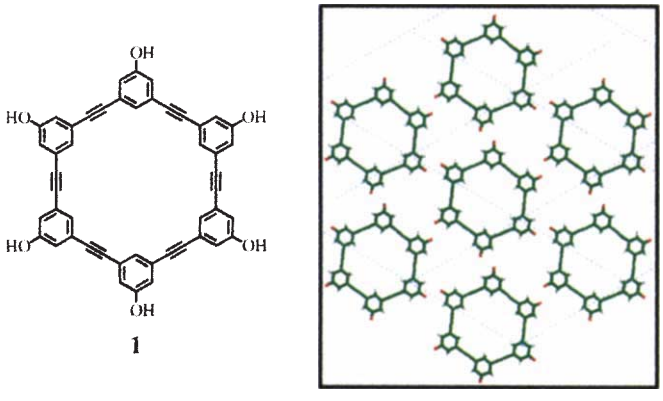

FIG. 1 Left, molecular formula of compound **1**. Right, single layer motif from the crystal structure of **1** parallel to the (001) plane. The macrocycles form a two-dimensional hexagonal closest packing stabilized by hydrogen-bonding interactions. Included solvent molecules have been removed for clarity.

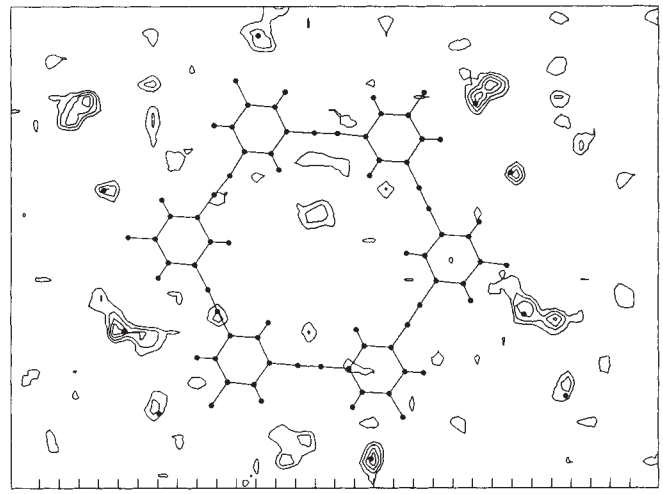

FIG. 2 Difference Fourier diagram for **1** (projected along the mean plane passing through atoms of the macrocyle) before the solvent molecules were added to the model. The peaks in the difference Fourier map coincide with the positions of the oxygen atoms of the solvents in the final model.

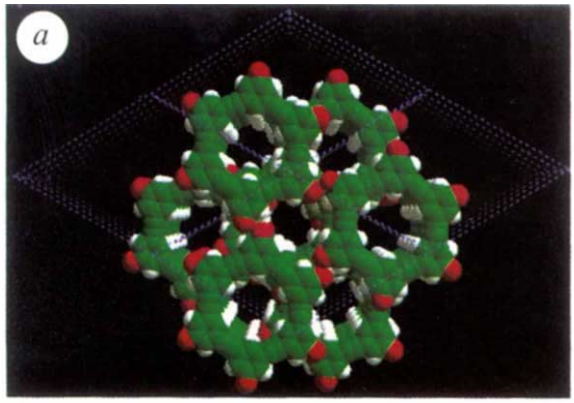

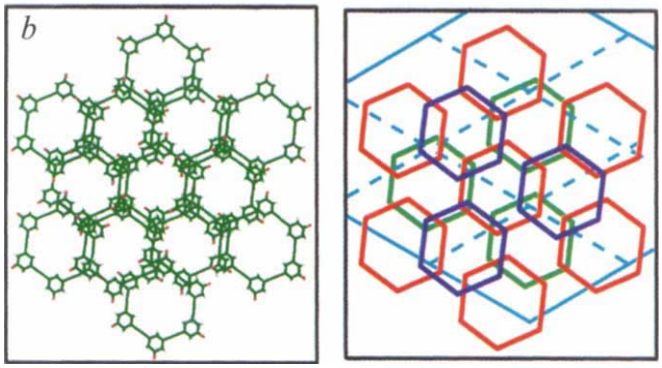

FIG. 3 *a*, Space-filling rendition of **1** viewed along the [010] axis. Extended channels with a diameter of ~9 Å are clearly visible. *b*, Packing diagram of three layers viewed along the [010] axis (left) and a schematic showing their relative arrangement (right). With reference to Fig. 1, the central hexagon in the middle layer (red) has a total of 12 nearest neighbours (6 in the same layer, 3 in the upper layer (blue), and 3 in the lower layer (green). The layers are stacked in the sequence . . . ABCABC . . . of cubic closest packing.

to optimize hydrogen bonding. The stack mode further benefits from efficient van der Waals contacts and electrostatic interactions between aromatic rings in adjacent layers (see below). Each hydrogen-bonded motif (without the solvents) in a sheet could be described according to Etter's terminology as an R_3^3 (32) graph set[25]. The O–O distance between two hydrogen-bonded phenols is 2.69 Å and the angle C–O–O is 117.2°. If we were to assume a geometrically calculated position for the hydrogen atoms, whereby the C–O–H angle is 120° (C–O–H angle in hydroquinone by neutron diffraction was found to be 121.0°), then the O–H---O angle of the hydrogen bond is 175.4°, very close to the optimum value of 180° (ref. 26). To achieve this optimum hydrogen bonding, there is a slight twist in the macrocycles with respect to the *a* axis. Each sheet has two types of holes: (1) the 9-Å hole generated by the macrocycle and (2) the 9.3-Å hole generated by the hydrogen bonds. Each of these cavities is filled with solvent molecules which hydrogen bond to the macrocycles and with one another. Methyl and methylene groups from the solvent molecules fill space in the cavities of adjacent layers, as well as in the layer from which they originate. The sheets are separated by 3.33 Å and stack in an . .ABCABC. . sequence of cubic closest packing, identical to that of β-graphite[37]. This stacking aligns the macrocycles in such a way as to generate an extended channel 9 Å in diameter running parallel to the *c* axis (Fig. 3*a*). Proper registry between macrocycles in adjacent layers is crucial for extended channels. This alignment seems to be achieved by van der Waals and electrostatic interactions between aromatic rings of adjacent layers. The slight lateral offset between aromatic rings seen in Fig. 3*b* is a common feature of the stack pattern and has been attributed to optimization of electrostatic interactions (minimization of π–π electron repulsion and maximization of the interaction of positively charged hydrogen atoms of one ring with the negatively charged π-electrons of an adjacent ring)[24]. Each macrocycle has six nearest neighbours in a layer and three from each of the adjacent layers, making a total of 12 macrocycles at van der Waals distances (Fig. 3*b*). If we were to represent each molecule as a sphere located at the centre of the macrocycle, the structure reduces to that of a face-centred cubic arrangement. Because of the large holes within the macrocycles, the framework atoms only occupy about half the total cell volume. The remaining void space is largely filled with solvent molecules.

The synthesis of new macrocycles opens up a number of possibilities. Because sections of the desired channel are pre-assembled with covalent bonds before crystallization, the size and shape of the channel's cross-section are dictated by the macrocycle's inner geometry. Also, as the organic building blocks can be readily modified, one can in principle tailor the microscopic cavity environment. Work is in progress to incorporate metal-coordinating functional groups to assemble binary organic–inorganic networks with concomitantly stronger intermolecular bonds. □

Received 16 May; accepted 15 September 1994.

1. Ozin, G. A., Kuperman, A. & Stein, A. *Angew. Chem. int. Edn engl.* **28,** 359–376 (1989).
2. Rolinson, D. R. *Chem. Rev.* **90,** 867–878 (1990).
3. Zerkowski, J. A., MacDonald, J. C., Seto, C. T., Wierda, D. A. & Whitesides, G. M. *J. Am. chem. Soc.* **116,** 2382–2391 (1994).
4. Chang, Y. L., West, M. A., Fowler, F. W. & Lauher, J. W. *J. Am. chem. Soc.* **115,** 5991–6000 (1993).
5. Lehn, J.-M., Mascal, M., DeCian, A. & Fischer, J. *J. chem. Soc., Perkin Trans. 2* 461–467 (1992).
6. Garcia-Tellado, F., Geib, S. J., Goswami, S. & Hamilton, A. D. *J. Am. chem. Soc.* **113,** 9265–9269 (1991).
7. Etter, M. C. & Adsmond, D. A. *J. chem. Soc., chem. Commun.* 589–591 (1990).
8. Michaelides, A., Kiritsis, V., Skoulika, S. & Aubury, A. *Angew. Chem. int. Edn engl.* **32,** 1495–1497 (1993).
9. Simard, M., Su, D. & Wuest, J. D. *J. Am. chem. Soc.* **113,** 4696–4698 (1991).
10. Ermer, O. & Eling, A. *Angew. Chem. int. Edn engl.* **27,** 829–833 (1988).
11. Ermer, O. & Lindenberg, L. *Helv. chim. Acta.* **74,** 825–877 (1991).
12. Hoskins, B. F. & Robson, R. *J. Am. chem. Soc.* **112,** 1546–1554 (1990).
13. Duchamp, D. J. & Marsh, R. E. *Acta Crystallogr.* B**25,** 5–19 (1969).
14. Abrahams, B. F., Hoskins, B. F., Michail, D. M. & Robson, R. *Nature* **369,** 727–729 (1994).
15. Davies, J. E., Kemula, W., Powell, H. M. & Smith, N. O. *J. incl. Phenom.* **1,** 3–44 (1983).
16. Weber, E. *Molecular Inclusion and Molecular Recognition-Clathrates I* (ed. Weber, E.) 1 (Topics in Current Chemistry Vol. 140, Springer, Berlin, 1987).
17. Abbott, S. J. *et al. J. chem. Soc., chem. Commun.* 796–797 (1982).
18. Weber, E., Pollex, R. & Czugler, M. *J. org. Chem.* **57,** 4068–4070 (1992).
19. Ghadiri, M. R., Granja, J. R., Milligan, R. A., Mcree, D. E. & Khazanovich, N. *Nature* **366,** 324–327 (1993).
20. Zhang, J., Pesak, D. J., Ludwick, J. L. & Moore, J. S. *J. Am. chem. Soc.* **116,** 4227–4239 (1994).
21. Zhang, J. & Moore, J. S. *J. Am. chem. Soc.* **114,** 9701–9702 (1992).
22. Zhang, J. & Moore, J. S. *J. Am. chem. Soc.* **116,** 2655–2656 (1994).
23. Sheldrick, G. M. *Crystal Solution Program* (Inst. fuer Anorg. Chemie, Gottingen, 1993).
24. Desiraju, G. R. *Crystal Engineering* 92–101 (Elsevier, New York, 1989).
25. Etter, M. C. *Acc. chem. Res.* **23,** 120–126 (1990).
26. Boeyens, J. C. A. & Pretorius, J. A. *Acta crystallogr.* B**33,** 2120–2124 (1977).
27. Greenwood, N. N. & Earnshaw, A. *Chemistry of the Elements* 304 (Pergamon, Oxford, 1986).

SUPPLEMENTARY INFORMATION. Requests for a complete set of atomic coordinates and crystallographic details should be addressed to Mary Sheehan at the London editorial office of *Nature*.

ACKNOWLEDGEMENTS. We thank J. W. Kampf for collecting the data for this crystal and S. R. Wilson for a copy of the SHELXL-93 program. J.S.M. thanks the US NSF, the NSF Young Investigator programme (1992–97) and the 3M company (non-tenured faculty awards programme) for their support. S.L. thanks the A. P. Sloan Foundation, and the J. D. and C. T. MacArthur Foundation for fellowships.